OBSERVING FLUID TRANSPORT INTO POROUS COATING STRUCTURES: SOME NOVEL FINDINGS

P. A. C. Gane
Vice President Research & Development
Paper & Pigment Systems

J. Schoelkopf*
Senior Scientist

D. C. Spielmann
Paper Research Group Leader

OMYA, Plüss-Staufer AG
CH-4665 Oftringen
Switzerland

G. P. Matthews
Reader in Applied Physical Chemistry

C. J. Ridgway
Post Doctoral Research Fellow

Department of Environmental Sciences
Fluid Interactions Research Group
University of Plymouth
PL4 8AA Devon, U.K.

ABSTRACT

This paper discusses novel methods for observing the spreading and penetration behaviour of fluids into specially prepared consolidated blocks of paper coating pigments which allows for the equilibrium absorption of measurable droplet sizes without saturation of the pigment layer. The mechanisms studied are responsible for a range of printing phenomena. Variables such as particle size distribution, pigment surface treatment with dispersing agents and the applied pressure during consolidation of the structure give the possibility to create a wide range of porous structures with differing structure-property relationships. By bringing liquids of differing polarity, surface tension and viscosity, stained and unstained, into contact with these porous blocks, either as a super source or in droplet form, the relevant phenomena of spreading, penetration and adsorption can be studied using image analysis techniques. Droplet absorption and pressureless fluid imbibition methods are contrasted to study the influence of surface free energy of the solid and liquid phases in combination with a given pore system and modelled geometry evaluated using mercury porosimetry and a pore structure modelling software (Pore-Cor). This software generates a three-dimensional pore network matching the experimental percolation characteristics and porosity, and giving some characteristic structural parameters modelling the structure in terms of pores and access throats. Results show that there is a discontinuity in the relationships between relative compaction, pore size distribution and the volume of liquid absorbed as a function of penetration depth which in turn can be significantly less than the volume measured by intrusion porosimetry in the case of droplet imbibition compared with saturation by super source imbibition. Identifying that this discontinuity cannot be readily modelled with the simple geometry of cubic pores with cylindrical connecting throats provides for potential mechanisms to be postulated and the future studies necessary to test these mechanisms to be defined. In practice these discontinuous absorption volume controlling mechanisms are seen as contributing factors to the different offset printing properties of gloss and matt papers in relation to fountain solution absorption and ink tack development and decay, and hence print abrasion, and when inhomogeneously distributed on a coated surface may be one of the most common causes for print mottle in modern coated papers.

Keywords: Pigment packing, porosity, pore modelling, liquid absorption, paper coating, penetration, printability

* Author to whom correspondence should be addressed

INTRODUCTION

The basics of fluid/porous solid interactions are fundamental to many natural and industrial processes. Many desired and undesired phenomena are dependent on the dynamics of this process and it continues to challenge many researchers to investigate paper absorption mechanisms in further detail. A major requirement for paper is a uniform distribution of the absorption controlling parameters over the surface otherwise a pattern of different print density or gloss becomes obvious as a mottling effect (1, 2).

In the manufacture of paper, pigments for coating and filling hold one of the key functions in the processes of adsorption, spreading and absorption into the porous structure. When a droplet of printing ink, e.g. from an office ink jet printer, comes onto the paper surface the final printing result in terms of colour setting, intensity and detail accuracy is strongly dependent on how far the droplet penetrates in connection to the spreading on the paper and where the ink pigment particles or dyes are deposited and in which time order this happens (3, 4, 5, 6, 7, 8, 9, 10, 11).

In previous studies many contributing factors have been analysed. In general, the approach has been based on porosity and pore size distributions obtained using mercury intrusion porosimetry (12, 13). When using this method two limitations should be corrected in the case of coating structure analysis as described by Gane et al. (14), namely, the compressibility of the sample and more importantly the shielding effect of small pores or throats which can prevent the intrusion of mercury at a given pressure into a pore of relevant size according to the straightforward Laplace equation. The porosity itself gives insufficient information about liquid uptake characteristics. A primary determining factor for non-pressure driven imbibition is the contact angle and therefore the interfacial energy relationships between the imbibed fluid and the microscopic surface continuity/discontinuity of the pore structure network. If the solid surface adhesion forces to the liquid are much weaker than the fluid cohesivity, resulting in a locally high contact angle, pore entry may be prevented even for very porous samples. Direct measurements of solid surface free energy on the truly microscale are extremely difficult. In the literature many attempts are reported to study wetting characteristics through the related contact angle (15) but in reality they are influenced by surface roughness, adsorbed materials, contamination and crystallite orientation. Among others, also inverse gas chromatography (16), cleavage energy (17) and a thin-layer wicking technique (18) have been used to obtain further information on this topic. Additionally, it is postulated here that in the case where the cohesivity within a fluid is weaker than the adhesivity of the fluid to the solid substrate, the potential for exceeding the yield point of the meniscus is given and the fluid progress into the structure is controlled by competitive imbibition.

The rate of offset ink tack increase is a common measure of ink solvent removal by the paper and the subsequent ink curing (19, 20). More recently, ink particle and dye deposition have also been studied, mainly related to ink jet applications, considering chromatographic separation of the ink (5). Also attempts to link light scattering properties to porosity measurements are reported (1, 21).

Oil absorption has been contrasted to mercury porosimetry to support the use of intrusion methods to describe the relevant pore structure of a coating for imbibition (22, 23, 24, 25). One problem which we identify from our study here is the definition of the oil, particularly the degree of non-polarity, and this is discussed in respect of a super source method which samples the pore volume accessed by a variety of liquids. Although not affecting the results in this study it may impact some important solid-liquid interactions.

Many valuable investigations have been performed directly on paper surfaces or on model coating layers. However, if we consider that a paper coating has a thickness, depending on grade, of between 5-15 µm, and a practical single ink layer is typically 0.25 µm (or in total on a four colour press ~1µm), it is to be expected that using even volumes as small as a micro litre directly onto such a microscopic surface volume is distinctly limited by saturation phenomena when it comes to understanding the complexities of coating imbibition. We decided to step away from thin coating layers, because of these

limitations, and to consider the possibility of using macroscopic blocks of consolidated pigment formed over a range of compressions which allow for the equilibrium absorption of measurable droplet sizes without saturation. It has been possible to investigate in detail the competition between surface spread and capillary absorption and the relationship of initial pore filling to factors such as surface chemistry and geometry of the pigmented pore structure as a function of sample compression.

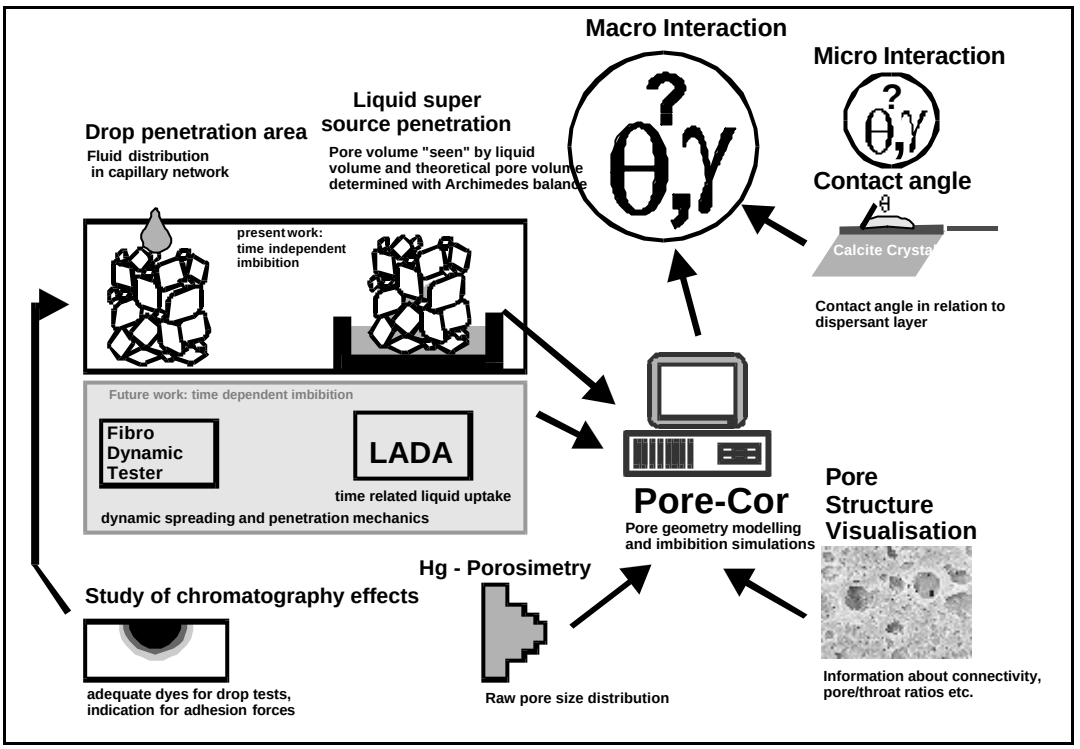

Fig. 1 Schematic of the overview of the present and future approaches used in this work.

Combining the findings of the droplet and the super source method and by contrasting them to the results of mercury porosimetry our target is also to advance the existing Pore-Cor† software (26) to a stage where three-dimensional pore geometry together with discontinuous pore wall surface energy distribution is modelled to simulate natural fluid imbibition and separation characteristics - as summarised in Fig. 1. In the present state the Pore-Cor model fails to predict discontinuous phenomena reported in this work. These findings are used to discuss the likely origins of the novel findings and proposals are made for the future modification of the model to elucidate these mechanisms.

SPREADING AND ABSORPTION MECHANISMS

Generally when a droplet of liquid contacts a porous surface two competing mechanisms start to act: spreading on the exposed surface and penetration/absorption into the porous structure. The distribution and wet adhesion of the fluid phase on the solid material at and within the porous structure surface are determined by many factors (27). Any force that acts at the microscopic interface between fluid and solid will influence the characteristic behaviour of spreading on a microscopic surface. The geometrical arrangement of these microscopic surfaces combine to control the spreading seen on the macroscopic scale. The same forces interact also with the fluid on the capillary walls of the mutual pore system and determine the penetration micro mechanics which couple together with the geometrical parameters of the capillary network to

† Pore-Cor is a software name of the Porous Media Research Group of the University of Plymouth, U.K.

determine the larger scale pore filling characteristics. The right balance between spreading and penetration/absorption influences whether the desired process will be successful or not. Details describing solid/liquid interactions are found in the literature (17, 28, 29). For example, so-called ink bottle pores do not allow the air to escape as liquid enters. Also, if the liquid meniscus curvature determining the driving Laplace pressure,

$$\Delta P = \frac{2\,\gamma\cos\theta}{r_{capillary}} \qquad \text{(eq. 1)}$$

where γ is the surface tension of the liquid and θ is the contact angle, is equal to zero, no capillary entry occurs. In this situation within a porous structure no further imbibition proceeds without applying an external pressure gradient. Pores with strong diverging wall geometries may act as imbibition stoppers or lead to a splitting of the wetting liquid penetration front (30). Many extreme configurations are imaginable which terminate the capillary uptake but in reality are assumed to be of negligible importance due to small edge defects and roughnesses which are always present in real systems.

CHOOSING TEST LIQUIDS

A review of recent publications (31, 32) on printing inks and the study of standard tests indicates the following main liquid components of printing inks:

	Rotogravure	Flexo	Offset	News	Ink Jet
Solvents and oils	Toluene Xylene Ethylacetate	Water Ethanol Ethyleneglycol Propyleneglycol Ethoxy- and methoxy-propanol	Saturated short Alkanes from Mineral oil fractions Linseed oil	Mineral oils *new*: Oils from soy and linseed	Water Ethylene-glycol Diols Pyrolidone
Solid components (waxes and resins)	Polyethylene Waxes Natural Resin Talloresin Nitrocelluloses Maleic-polyacrylic-vinyl resins	Maleic-, polyamide-, vinyl resins	Monoester of Fatty acids Alkyd resins	Waxes Bitumen derivates Natural resins	
Dyes		Alkali dyes			Direct dyes Acidic dyes

Table 1 Overview of typical ink compositions [ink pigment size is in the range of 0.05 - 0.5 µm].

Many of these fluids are blends of different sub-components. Some of them contain dissolved or dispersed solids. Of each family of liquids we chose one typical representative in its chemically pure form. These are shown in table 2 together with some additional liquids with typical values in surface tension, viscosity and polarity selected to cover the imaginable range of fluids likely to absorb into a pigment layer. To complete the table, viscosity and surface tension of some of the relatively unknown fluids were measured in the lab (*). Viscosity was determined with a StressTech®‡ rheometer performing a small ramp of shear rates. Surface tension was measured with a Krüss Digital Tensiometer K10T.

‡ StressTech® is a product name of ReoLogica Instruments AB, Lund, Sweden

	Surface tension / mN/m	Viscosity at room temperature / mPas	Dielectric constant	Boiling point / °C	Polarity
Water	72	1.056	80.18	100	high
Glycerol	63	1490	42.5	138-140	medium
Ethyleneglycol	48	19.9	37/25	195-197	medium
Linseed oil (*)	35	33.1	n.a.	n.a	medium
Toluene	29	0.71	2.379/25	110-111	low
Squalane (*)	29	38.8	n.a.	350	very low
Nonane	22	0.59	1.972/20	150-151	negligible

Table 2 Properties of the test fluids.

Squalane (2,6,10,15,19,23-Hexamethyltetracosan, Perhydrosqualane) a derivate of an extract from shark liver was chosen because it is one of the few available long-chain liquid alkanes of medium viscosity which is chemically pure.

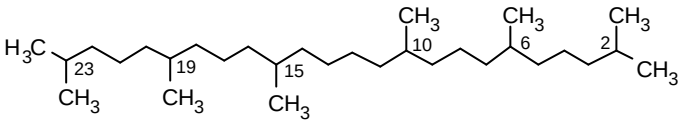

Fig. 2 Chemical structure of squalane.

Linseed oil was chosen to represent a vegetable oil relevant to the recent revival of the use of natural oils in printing ink formulations (33). Because its main components, namely triglycerides of linolic-, linoleic- and oleic-acid, are uncommon in chemically pure form we chose to work with the natural oil. An important difference to typical aliphatic alkane-based mineral oil is the more polar (dipole) character due to the double bonds and carboxy groups (Fig. 3). In the context of this work, the term apolar is therefore only used for the aliphatic alkanes.

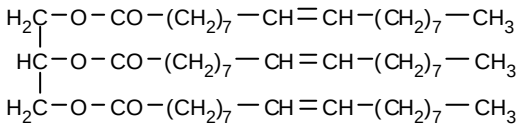

Fig. 3 Chemical structure of trioleine, triglyceride of oleic-acid.

Toluene is included representing the typical rotogravure solvent. *Ethyleneglycol*, as a component of flexo inks, is one of the few liquids with a surface tension within the mid-range of ~ 40-50 mN/m.

The dipole moments of the liquids can be measured over a specified range of oscillator frequencies, but values are not generally available. The polarity of the bulk liquid is a less well-defined term associated with dipole moment, but is also dependent on other properties such as molecular polarisability, intermolecular hydrogen bonding and the entropy of the liquid (34, 35). A useful qualitative estimate of polarity can be made by inspection of the molecular structure. The small size and large dipole moment of water molecules give the liquid a high polarity. The substituent groups within glycerol, ethyleneglycol and linseed oil give these liquids a medium polarity. In squalane, the small local dipole moments of the methyl groups, together with the random C-C orientations within the backbone of the molecule, give it a very low but non-zero overall polarity. The polarity of nonane, which has no substituent groups, is caused only by distortions of the carbon backbone and is therefore negligible.

EXPERIMENTAL TECHNIQUES AND RESULTS

Preparation of dry pigment tablets

A method has been developed to investigate the spreading and penetration behaviour of fluids as used in the printing of coated paper, derived from an extension of the preparatory work of Schoelkopf in support of the studies made by Penannen (36), in which macroscopic blocks of mineral coating pigments are formed. The formation of compressed structures was also described by Ridgway et al. (37) for lactose.

For the preparation of these pigment blocks a cylindrical hardened steel die attached to a baseplate with a single acting upper piston is used which is suitable for a wide range of pigment particle sizes, chemistries and morphologies. The die is divisible into two parts to aid removal of the compacted pigment sample and the walls of the die are protected with a strip of plastic film to prevent sticking of the powder to the wall and to reduce edge friction (Fig. 4).

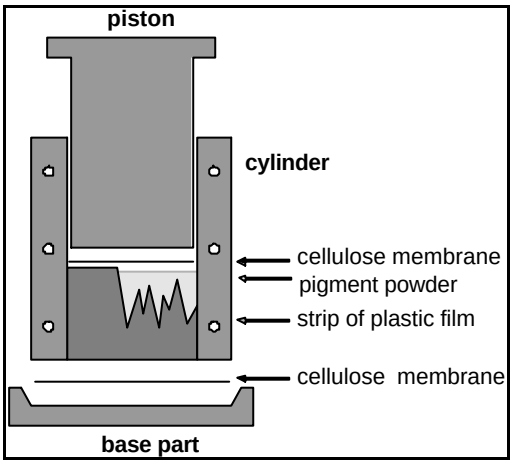

Fig. 4 Schematic cross-section of the die showing the plastic lining and cellulose membrane.

Briscoe and Rough (38) reported non-uniform packing densities in highly compacted powders induced by wall friction effects. For this study we considered this effect to be negligible because of the relatively lower pressure ranges adopted here and the broader particle size distributions of coating pigments result fortuitously in a certain micro-heterogeneity of the tablet. This micro-heterogeneity in turn accommodates for likely stress release within the tablet leading to a macro-homogeneity which is clearly monitorable by the droplet shape on the tablet surface after the surface is carefully formed by grinding the block such that the inner structure is revealed.

We concentrate our report here on the use of a spray dried predispersed natural ground calcium carbonate derived from limestone with a particle size distribution of 91 wt% < 5 µm, 55 wt% < 2 µm, 30 wt% < 1µm. The pigment was equilibrated in an atmosphere of 100% relative humidity at 23°C prior to tablet formation. Each tablet is formed from 60 g of homogenised powder carbonate. The homogenising must be carefully controlled and performed under consistent conditions. The pigment is then compacted in an hydraulic press for 5 minutes at a predetermined pressure. The range of applied press forces F, the press area A, and the resulting pressures are listed in table 3.

Cross-sectional area, A = 17.35 cm^2 (±0.16)	
Applied force F / kN (±5)	Effective pressure P / MPa (±2.7)
100	57.6
200	115.3
300	172.9
400	230.6
450	259.4

Table 3 Conversion table of applied forces to resulting pressures.

Mercury intrusion porosimetry

The mercury intrusion data were obtained from each block sample on a Micromeritics Autopore III porosimeter using the technique described by Gane, Kettle, Matthews and Ridgway (14) up to an applied pressure of 415 MPa. In this method the intrusion data are corrected using a spreadsheet-based program Pore-Comp [§] which uses a blank run correction with the Tait equation (39) to correct for mercury compressibility and penetrometer expansion effects. A novel aspect of the spreadsheet is that it can also be used to correct for, or to determine, any compression of the solid phase of the sample which may occur at high intrusion pressure.

The final corrected data from Pore-Comp are formed into a matrix containing the pore diameter, which was obtained using the well-known Laplace equation, the corresponding percentile pore volume and the intrusion volume in cm^3/g. These then form the input data for the Pore-Cor model software which simulates the three-dimensional void space structures matching the experimental percolation characteristics and porosity using the description of pore networks involving pores and access throats - the simulation match is seen to be quite acceptable from the correlations shown in Fig. 5 and Fig. 6.

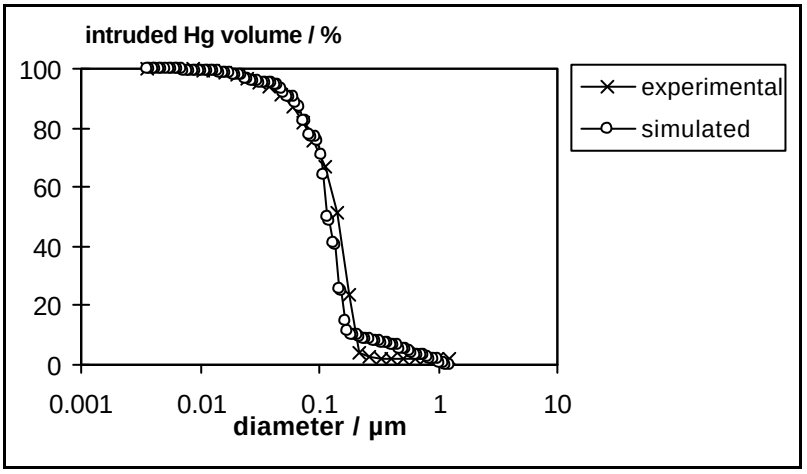

Fig. 5 Experimental and simulated percentile mercury intrusion volume from a tablet consolidated at 57.6 MPa.

[§] Pore-Comp is a program software name of the Porous Media Research Group at the University of Plymouth, U.K.

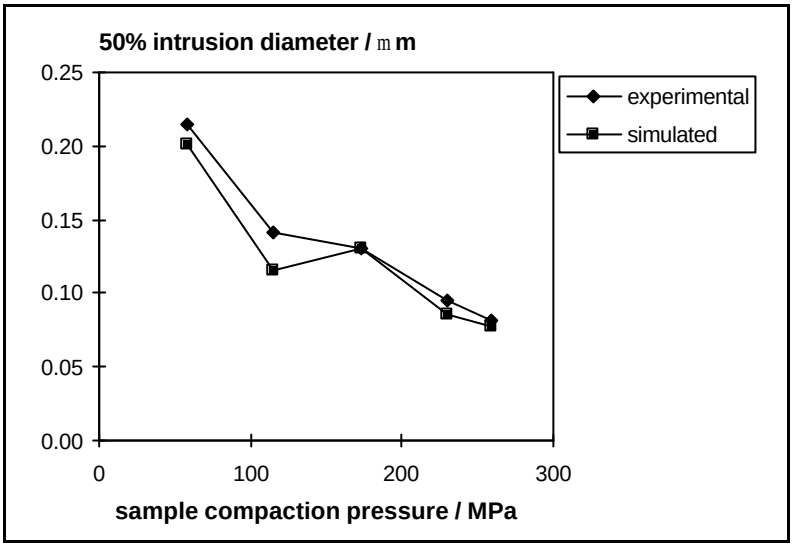

Fig. 6 Experimental and simulated 50 % mercury intrusion data show that the mean pore diameter (and porosity) decrease as a function of increasing sample formation pressure.

We also see in Fig. 6 that the intrusion diameter is not necessarily a smooth function of sample compaction pressure neither in the experimental nor in the corresponding simulated curves where the slight deviation in the experimental curve is somewhat more pronounced by the simulation attempting to match percolation data. At this stage the significance of the simulated discontinuity is not further investigated as the following discussion suggests that the model requires modification rather than it providing insight into this phenomenon. It is on this basis that the following analyses were made considering experimental porosity as the independent variable and not external sample compression.

SUPER SOURCE SORPTION

The super source imbibition method is used as a simple porosity method to sample the imbibition void volume. The amount of liquid which can be taken up just by the capillarity of the porous system is measured without the influence of an external intrusion pressure. If a liquid were totally non-wetting then no liquid would be absorbed. The liquid is present in abundance and the sample small enough so that the differential between gravity and capillary pressure is negligible. Typically, a sample size of about 1 cm^3 is made by cleaving a pre-formed pigment tablet into approximately usable sized pieces with the help of a gentle tapping and cutting with a very sharp knife. The edges are honed with a sample grinding machine and a medium grit paper at 200 rpm. This finishing technique effectively removes artefacts that might have arisen during the sample breaking. The samples are weighed, labelled and put in a shallow glass dish which in turn is placed in a larger outer dish. The inner dish is filled with the fluid under investigation taking care to avoid splashes and false wetting of the sample. The filling height is just sufficient to ensure that every sample is in contact with the fluid - too high a fluid level can lead to trapped air in the samples and this must be stringently avoided. The dish is fitted with an overlip cover and the outer dish carefully filled with distilled water until it reaches the cover to give a complete vapour seal.

After complete soaking of the compressed sample block - often accompanied by a colour intensity change because of the reduced light scattering at the inter-particle boundaries - the sample is removed, superficially dried with a tissue and immediately weighed. When using the highly volatile solvents a very fast action is needed to avoid evaporative losses!

The volume of the sample is also determined in its soaked condition on an Archimedes balance. We saw that a polar displacement liquid led to a rapid disintegration of the sample. It is suspected that the polar fluid is absorbed faster then the

extrusion capability of the non-polar fluid. Therefore, to ensure that no further pore access is inadvertently sampled by the displacement fluid, only a non-polar liquid can be used. We used kerosene (density $\rho_{kerosene}$). The outer volume of the sample, V_{sample}, can be calculated:

$$V_{sample} = \frac{\text{apparent sample mass in kerosene}}{\rho_{kerosene}} \qquad \text{(eq. 2)}$$

To minimise the unavoidable errors due to evaporation and loss of small particles at the edges, every compaction level measurement was performed in triplicate.

A second independent form of volume can be obtained with this method so that by combining the Archimedes soaked volume, V_{sample}, (the outer volume of the sample) and the preweighed (M_{sample}) filled sample skeletal volume, $V_{skeleton}$, the internal pore volume, V_{pore}, can be calculated.

$$V_{pore}\,\% = \frac{100\left(V_{sample} - V_{skeleton}\right)}{V_{sample}} = f_{Archimedes} \qquad \text{(eq. 3)}$$

where

$$V_{skeleton} = \frac{M_{sample}}{\rho_{calciumcarbonate}} \qquad \text{(eq. 4)}$$

and $\rho_{calcium\ carbonate}$ is the assumed density of solid crystalline pigment. The absorbed mass of fluid, M_{fluid}, further gives the volume of pores accessed by the fluid of volume V_{fluid} knowing the fluid density ρ_{fluid},

$$V_{penetrated}\,\% = \frac{100\ V_{fluid}}{V_{sample}} = f_{penetrated} \qquad \text{(eq. 5)}$$

This last parameter, $V_{penetrated}$, is compared with the value of V_{pore} to determine the pore volume sampled by the imbibed fluid compared with the available pore volume.

In general, the porosity $\phi_{Archimedes}$ was found to be in good accordance with imbibition volume $\phi_{penetrated}$ for the test liquids. Mercury porosity also matches these findings (Fig. 7). [Note that the deviation of the last data point is unexplained and is assumed to be an artefact as the mercury intrusion measurement could not be repeated due to limited sample quantities.]

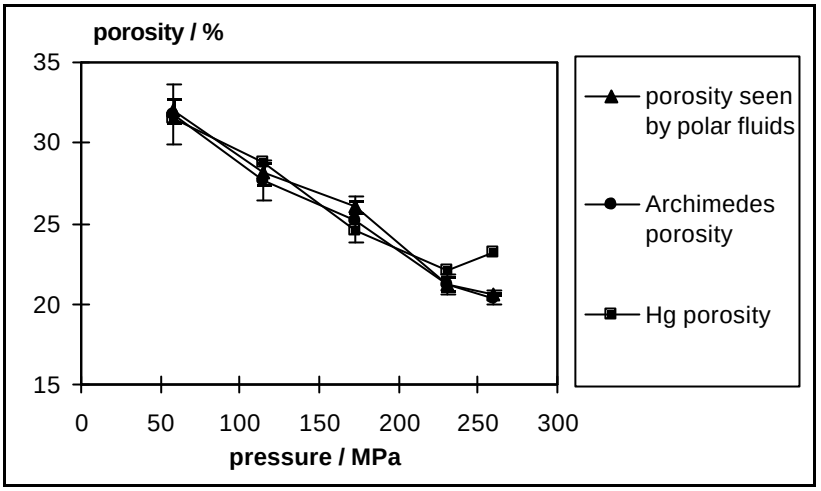

Fig. 7 Comparison of $\phi_{penetrated}$ for polar fluids, $\phi_{Archimedes}$, and mercury porosimetry ϕ_{Hg}

The complete set of penetrated (super source imbibed) porosities for all the liquids tested, as shown in Fig. 8, including water at two arbitrarily chosen porosities, is in direct correlation with the experimentally derived porosities over the sample compression range. We see that in the case of super source absorption, therefore, there is little or no differentiation between the case of apolar and polar liquids between the actual penetrated pore volume and the experimentally defined total available pore volumes.

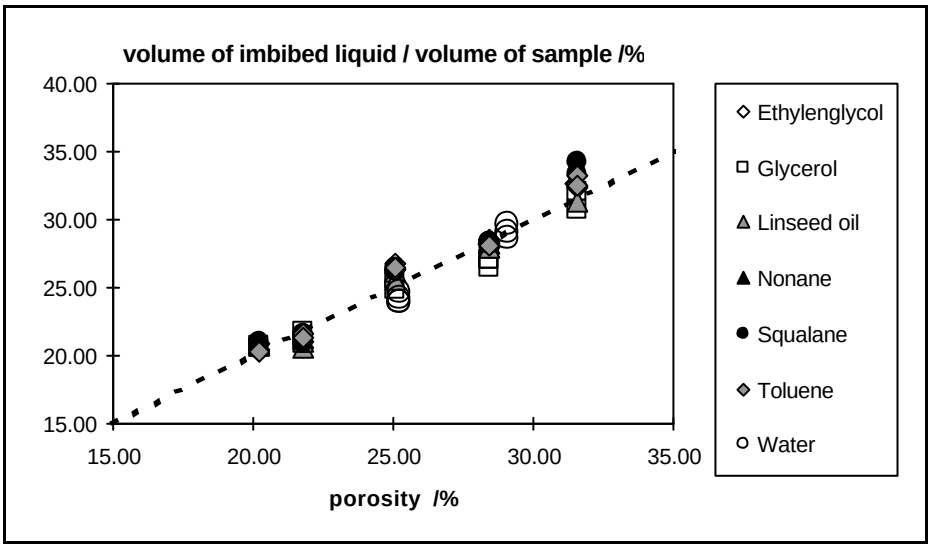

Fig. 8 One-to-one correlation of imbibed liquid volume with porosity for both the polar and apolar fluids as determined from the generalised correspondence shown in Fig. 7, including water at two arbitrarily chosen porosities.

These results[**] mirror the findings reported by Abrams et al. (12) and Leskinen (24), who found a good agreement between void volumes measured by oil absorption and mercury porosimetry.

As we discuss later, this total saturation effect as seen by super source is in marked contrast with the situation when the volume of liquid to be imbibed is limited in respect to the available pore volume of the sample, i.e. in the application of a

[**] These findings have been revised subsequent to the Proceedings of the Tappi Advanced Coating Fundamentals Symposium 1999 (43).

droplet or where the layer of fluid, such as contained in an ink layer, has insufficient volume to lead to saturation equilibrium of the sample.

DROPLET SORPTION - a discontinuous effect of compression on droplet penetration

This method is a direct approach to simulate on a macro-scale what is happening when a limited amount of dyed liquid is contacted upon a porous surface. Surface spreading acts in competition to the imbibition into the capillaries.

Selecting a suitable dye

Different aqueous dyes have been investigated for their suitability as an indicator for the liquid front. For this reason an experiment was made as described in the super source method in which the base surface of the sample block was brought into contact with underlying drops of different dyes to check the aqueous chromatographic behaviour of different dye molecules and ions through the slightly anionically dispersed calcium carbonate surface network.

All dyes with a cationic charge showed a strong adsorption to the calcium carbonate surface. This indicates that the ionic forces (Coulomb forces) contribute the strongest part of the adhesion force and is in agreement with findings covering ink jet dye adsorbing mechanisms (40). Acid dye molecules have a significantly weaker adhesion mechanism in which it is assumed that the COOH-groups probably interact with free surface of the Calcium Carbonate. Dyes with an anionic colorant revealed no adsorption onto the slightly anionically dispersed calcium carbonate surface. Therefore, we chose Aluminiumphthalocyanine-sodiumsulphonate as dye for our droplet test. The surface tension of the as-used solution of 1% was determined as 63 mN/m. An example of differential dye adsorption is shown in Pic. 1.

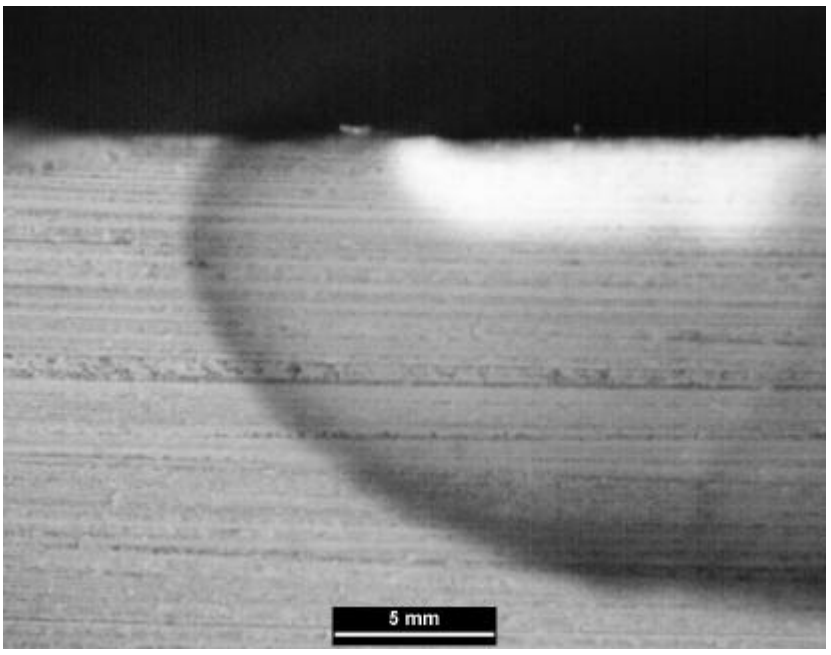

Pic. 1 The picture displays the cross-section view under the fluorescence microscope of the dyed tablet space of a blend of equal amounts of Rhodamin B (retarded) and Aluminiumphthalocyanine-sodiumsulphonate (advanced) and shows dramatically the chromatography effect. Magnification 50x.

Attempts to stain apolar solvents displayed a major problem because the interaction of a dye molecule with an alkane seemed always weaker than its affinity to a pigment surface which led immediately to adsorption and therefore to chromatographic separation of liquid and dye. For this reason we confined our investigation of absorption at this stage to aqueous systems.

Droplet application method

A droplet of 5 µl of liquid is formed at the tip of a gas-chromatic syringe. The drop is then carefully brought near to the surface of the tablet. When the drop touches the surface it is pulled by adhesion forces toward and onto the tablet surface. Every tablet is tested with at least 3 droplets - most of the experiments were made in quintuplicate. The tablet now with the surface droplet stains is placed on a normal Desktop Publishing Scanner (UMAX Powerlook II) and scanned with a resolution of 1400 dpi.

The spot shape or "roundness" is monitored as a form-factor which is calculated as the ratio of the minimum dimension to that of the maximum, i.e. $\text{diameter}_{min}/\text{diameter}_{max}$, and gives us information about the absorbed sample surface spread uniformity.

After equilibration for 24 h each sample dot on the compressed pigment tablet is subsequently ground in such a way that the cross section of the drop penetration at its largest lateral expansion could be scanned. With the help of an image analysis software package (KS 400, Kontron Electronic GmbH) the relevant parameters of surface spread area, shape, penetration cross-sectional area and penetration depth can be determined.

Obtaining a smooth surface and uniform spread

To check the influence of the surface roughness, a series of 4 tablets, each formed under a 100 kN press force, were surface ground in an automated grinding machine (Jean Wirtz, Phoenix 4000) with 4 different grinding papers: 60, 320, 1200, 2400 grit. The following graph (Fig. 9) shows the influence of the coarser grind paper grades on directional wetting and non uniformity due to surface scratches as illustrated by the example in Pic. 2.

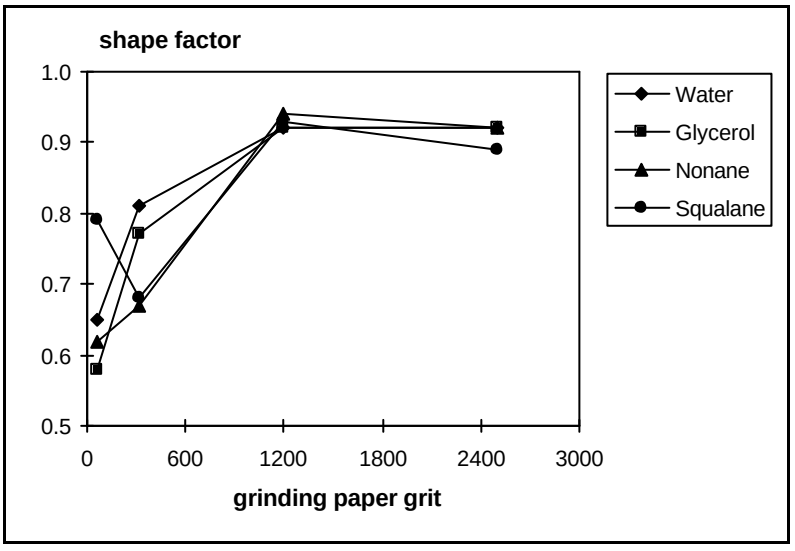

Fig. 9 With grit 1200, polished surfaces show maximum shape factor which means maximum roundness/uniformity of the droplet stain.

For all samples and all measured dots quoted here, the shape factor was 0.93 ± 0.01 which indicated that we had eliminated directionality and that pore access distribution and surface energy continuity are within usable limits.

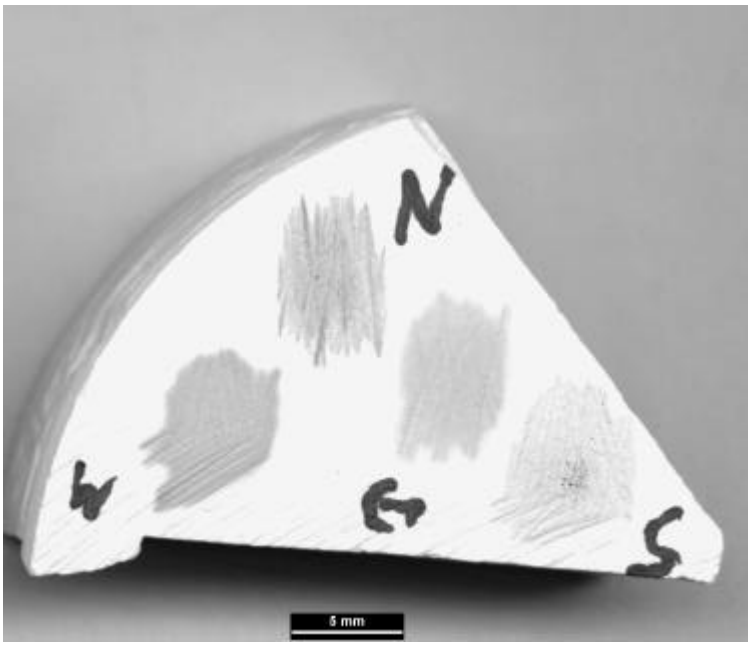

Pic. 2 Different stained liquids show strong influence of surface scratches (ground with 60 grit paper).

The humidity of the tablets also proved to be a very important factor. In the extreme case of a water-presoaked tablet, (Pic. 3), a drop of aqueous dye spreads to a large irregular dot (diameter > 10 mm) at very low penetration depth (< 0.5 mm). On the contrary an oven dried tablet (150 °C, 24 h) showed a higher surface wetting contact angle which resulted in a smaller dyed area and deeper penetration. We might explain this by the amount of hygroscopically adsorbed water normally present on the polyacrylate-based dispersant. The dispersant polymer requires the water for sufficient hydration to be electrostatically active and thus hydrophilic. It is known that if the water is evaporated by the influence of heat the polymer shrinks and covers much less particle surface.

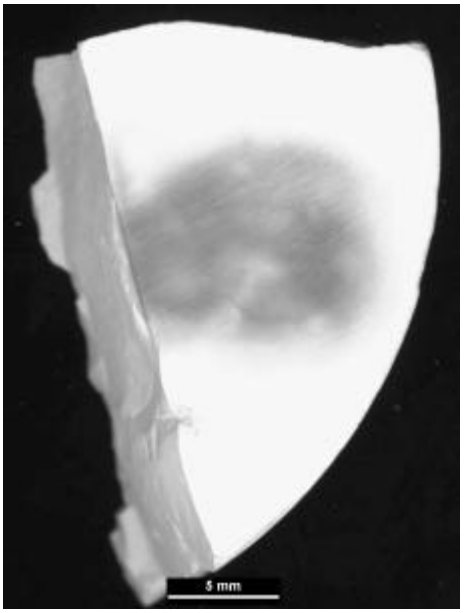

Pic. 3 Super source water-soaked tablet shows a blurred dyed droplet front.

For this study we decided to work under realistic climatic and humidity conditions such that, after consolidation, the tablets were equilibrated at 23 °C and 50 % relative humidity for more than 48 hours to a measured moisture content of 0.4 % to 0.8 %.

Observations and results

The process of primary absorption was generally so fast that no contact angle measurement was made. A second outer area of sub-surface spread was subsequently observed caused by internal horizontal capillary forces within the volume of the structure. This led to a ring of lighter colour around the initial spreading area when observed from above (Pic. 4). This fundamental observation told us that, in general, our surface structure must be also representative of the internal volume structure and had not been altered chemically or physically to create spread without a corresponding isometric imbibition.

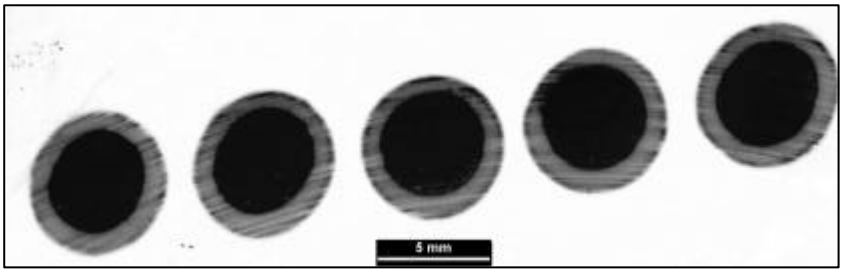

Pic. 4 Droplet dots on tablet surface.

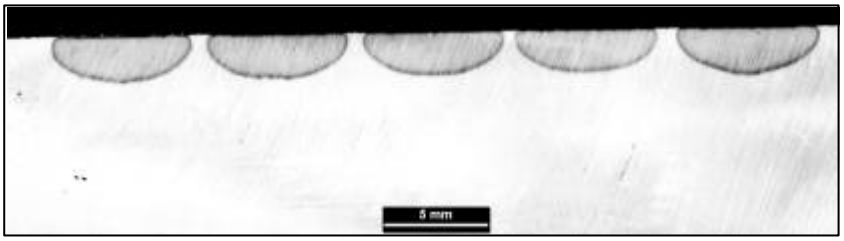

Pic. 5 Droplet dots viewed in cross-section after grinding.

The ratio between surface spread and absorption was calculated as the ratio of the mean surface diameter: maximum penetration depth (Pic. 5). Therefore, a high ratio means surface spread is favoured over penetration, and vice versa.

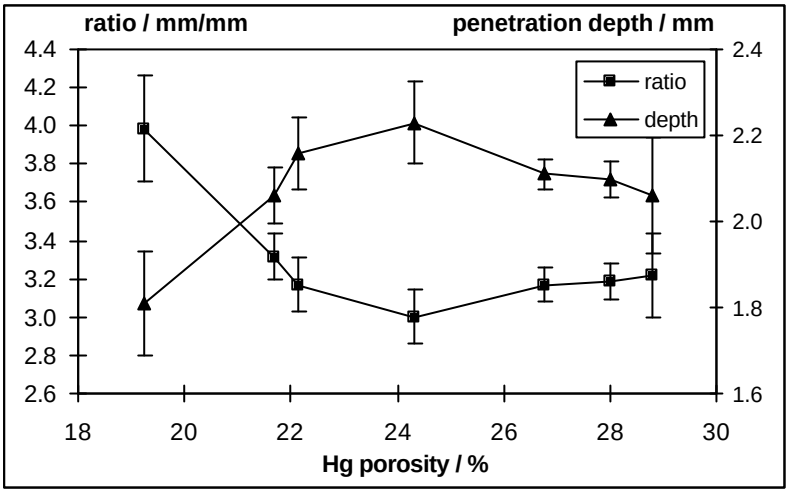

Fig. 10 Ratio of surface diameter to maximum penetration depth of a droplet shown as a function of the mercury porosity as measured from the identical series of compressed tablets.

Fig. 10 shows a transition in this ratio which is only consistent with the presence of unfilled voids. The individual penetration data indicate that there is an anomalously large penetration depth occurring as porosity increases. If all pores were filled (or remained filled) then the penetration depth of a highly porous structure should be less than that of a highly compressed structure. Since we are using a polar liquid (water) which we know from the super source data can access all pores, we must assume that any unfilled pores within the network should at least be surface wetted either by filling and subsequent draining or by diffusional adsorption of the liquid front.

To model this deviation from complete pore filling/drainage, a simulation program was written calculating approximate dimensions of rotationally symmetrical spheroidal segment volumes, $V_{simdyed}$, using parameters obtained from the corresponding image analysis data of the droplet test and contrasting them to a theoretical dyed volume, $V_{theodyed}$. By considering the applied volume of ink and the tablet porosity, the degree of unfilled pores can be detected.

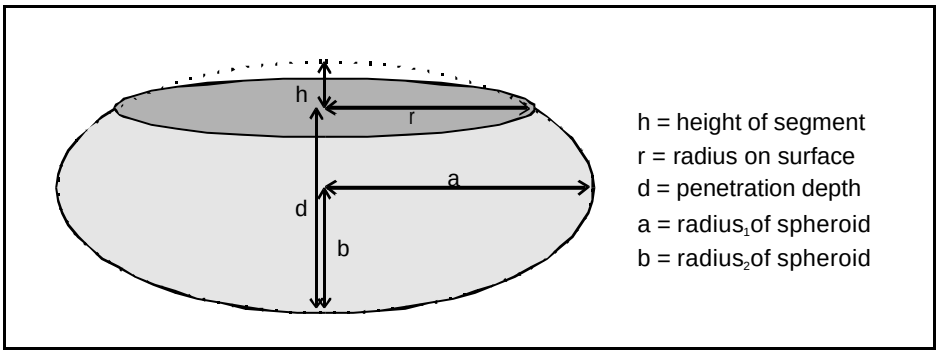

Fig. 11 Spheroidal approximation of the penetration volume.

The simulated penetration volume, $V_{simdyed}$, is calculated assuming the volume can be considered as part of a rotationally symmetrical spheroid having the two axes a and b,

$$V_{simdyed} = \frac{4\pi}{3} a^2 b - \frac{\pi h}{6}\left(3r^2 + h^2\right) \qquad \text{(eq. 6)}$$

where the volume, $V_{spheroid}$, for a complete spheroid would be

$$V_{spheroid} = \frac{4p}{3} a^2 b \qquad \text{(eq. 7)}$$

and the segment outside the penetration volume, $V_{simdyed}$, is subtracted as

$$V_{segment} = \frac{\pi h}{6}\left(3r^2 + h^2\right) \qquad \text{(eq. 8)}$$

The values for the spheroid radii, a, b, the surface radius, r, and the total penetration depth, d, are provided by the image analysing system and the height of the outer segment, h, is calculated using

$$h = 2b - d \qquad \text{(eq. 9)}$$

Further, a theoretical volume, $V_{theodyed}$, for the applied droplet within the structure is calculated as

$$V_{theodyed} = \frac{100\, V_{applied\ ink}}{\phi_{Hg}} \qquad \text{(eq. 10)}$$

Thus, comparing the two volumes $V_{simdyed}$ and $V_{theodyed}$ we see that the observed value is always far greater than the range where pores are simply filled with liquid (Fig. 12).

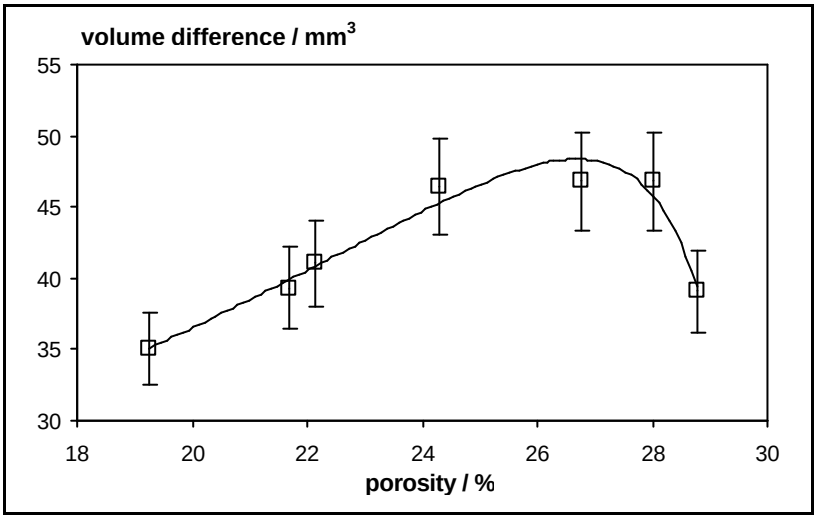

Fig. 12 The comparison of $V_{simdyed}$ and $V_{theodyed}$, expressed as difference ($V_{simdyed}$-$V_{theodyed}$), shows a marked transition as a function of the mercury porosity.

Pore-Cor modelling of the transition phenomenon

In the first instant after the droplet touches the surface a competition takes place between surface spread and capillary absorption forces. During this period super source conditions are momentarily present. In our case with the polar aqueous solution, we would have expected nearly complete pore filling should occur at this stage displacing air in the pore network. Either these assumed saturation conditions do not prevail during the short timescale initial absorption dynamics or, later, there may be a distinction between either locally different pore-wall wetting or adhesion, or through draining of larger pores into smaller pores or throats replacing liquid once again with air (provided the access to air is still ensured) or a potential meniscus fracture/retreat associated with strong film flow/wall wetting in a divergent pore, or a combination of all these possibilities.

In a natural polydisperse pore network with a multiplicity of geometrical configurations and irregularities this transition would not manifest itself as a sharp discontinuity in the penetration parameters but rather as a softer trend. However, it is possible to imagine that a complex combination of absolute pore diameter, pore-to-throat diameter ratio and connected throat void volume differential determines the competitive filling or drainage level of pores through connected throats.

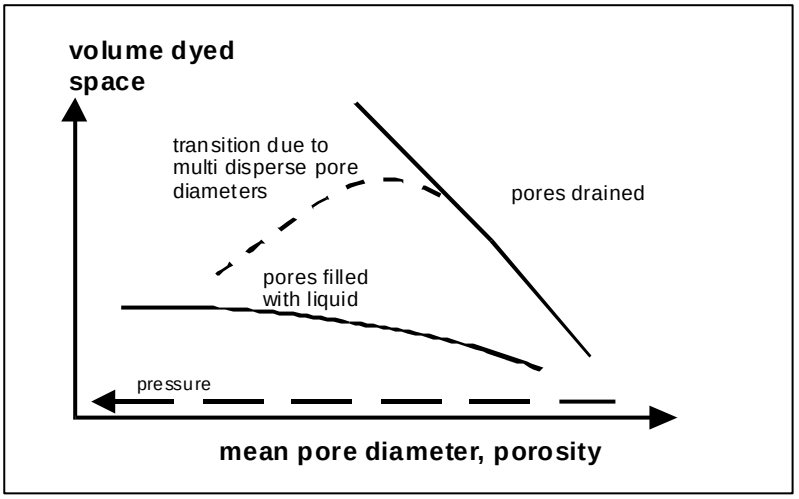

Fig. 13 Schematic showing the balance between total pore filling and either excluded pores or potential pore drainage/side-wall wetting.

At equilibrium, the competitive capillarity of fine versus large pores in a drainage model can be studied by the eccentricity or skew of the pore and throat diameters using the computational Pore-Cor. As an example, we include here the calculated parameters for the structures analysed in Fig. 6 as determined by Pore-Cor.

porosity (%)	**19.26**	**21.69**	**22.14**	**24.31**	**26.77**	**28.02**	**28.7**
dmin (µm)	0.004	0.004	0.004	0.004	0.004	0.004	0.004
dmax (µm)	1.21	1.21	1.21	1.21	1.22	1.22	1.21
pore skew	1.1	1.1	1.0	1.0	1.2	1.1	1.0
connectivity	3.5	3.4	3.2	3.3	3.4	3.4	3.2
throat skew	1.10	1.01	0.59	0.73	0.89	0.71	0.11
permeability (mD)	0.000307	0.000586	0.00145	0.00156	0.00122	0.00277	0.00915
tortuosity Q(1)	2.9	2.6	3.2	2.6	2.1	2.1	3.3
median	3.7	2.7	3.4	2.9	2.6	2.5	3.7
Q(3)	3.7	3.9	4.2	4.0	4.2	3	4.3
no of tortuosity runs	11	18	12	24	18	18	22
simulated d50 (µm)	0.078	0.086	0.13	0.115	0.102	0.133	0.201
experimental d50 (µm)	0.0814	0.0948	0.13	0.141	0.116	0.129	0.214
bulk density (g/cm^3)	2.18	2.14	2.07	2.02	2.00	1.97	1.87
skeletal density (g/cm^3)	2.74	2.81	2.72	2.72	2.76	2.80	2.72
total intruded volume (cm^3/g)	0.0942	0.1113	0.1153	0.127	0.1382	0.1505	0.1669

Table 4 Calculated parameters by Pore-Cor, showing the increase in throat skew as consolidation pressure increases.

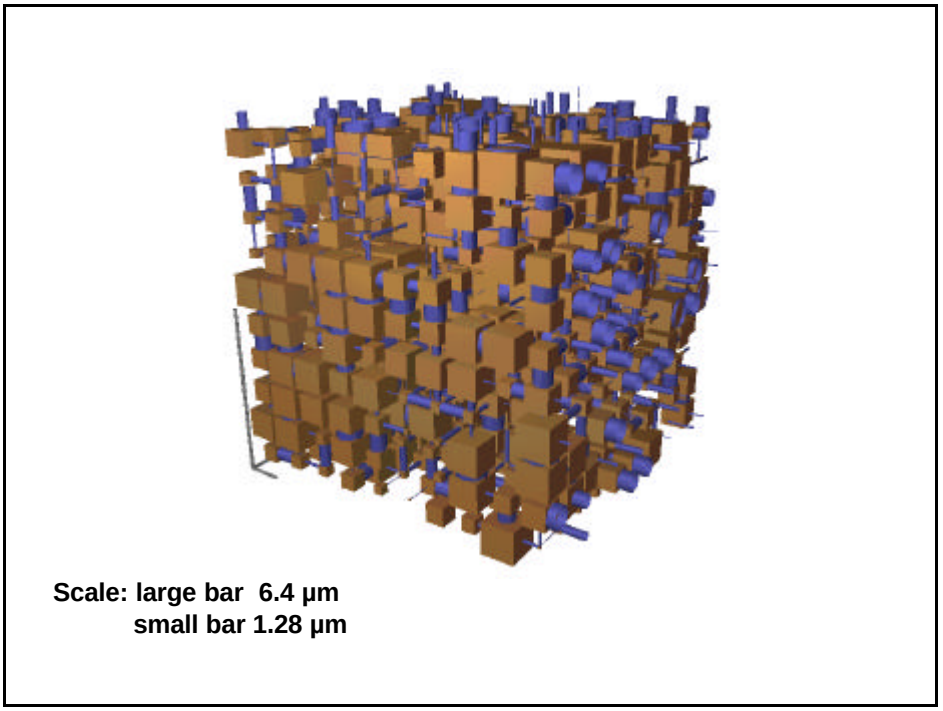

Fig. 14 Unit cell of a tablet consolidated at 57.6 MPa having a porosity of 28.7%

Fig. 14 shows a Pore-Cor model structure involving cubic pores and cylindrical throats. Since this porous structure has two size distribution parameters (Fig. 15), i.e. that of the pore sizes and that of the throats (skew), where the maximum throat diameter is limited to the size of the connected pore, we can search for discontinuities in the parameters which might correspond to the discontinuous sorptive behaviour. As can be seen in table 4, there is a continuous increase in throat skew but this alone cannot describe the observed sorptive discontinuity based on traditional criteria.

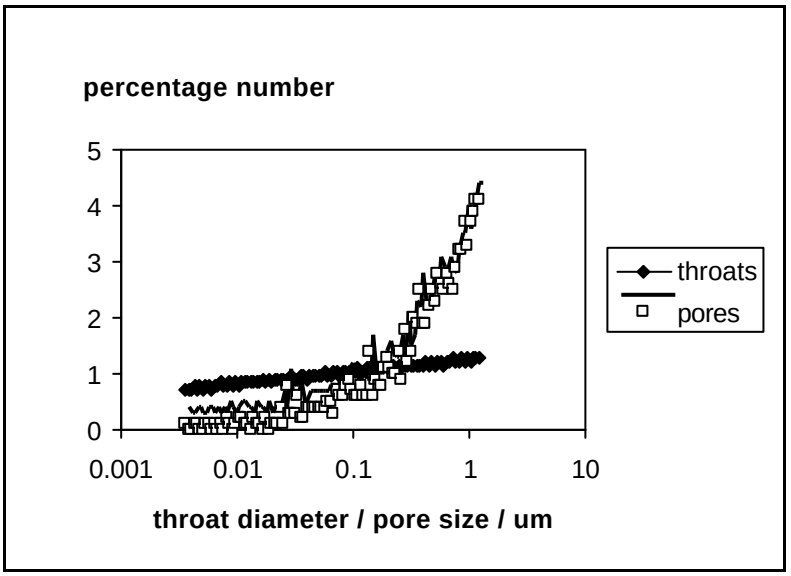

Fig. 15 Pore and throat diameter distribution for the structure shown in Fig. 14. (The percentage number represents the occurrence of the corresponding diameter).

Further developments of Pore-Cor can now account for diverging and converging throat geometries in association with surface energy which can be used to differentiate polar and apolar super source data in respect of unaccessed pore volume. In a final steady state development, a correspondence is sought between wall-wetting of certain pores to reveal an unfilled pore volume consistent with the observations from droplet absorption. The analytical details of this work together with time-dependent absorption studies will be the subject of future publications.

CONCLUSIONS AND IMPLICATIONS

A novel way of studying the comparative absorption under either super source saturation conditions or limited volume droplet imbibition has been presented. In the investigated pore structures, defined by using predispersed coating pigment tablets formed under differing compressions, transitional conditions were observed distinguishing the often studied saturation absorption from the more realistic limited volume case. These are summarised as:

1. In *super source* imbibition, corresponding to the situation of abundant fluid at all stages of absorption, the progress to complete saturation of the pore volume is independent of the range of fluid types studied and corresponds to the fully corrected mercury porosimetry values.
2. A transition/discontinuity was seen in the case of *limited volume droplet* imbibition where the ratio of droplet surface spread compared with absorption showed a marked deviation from complete pore filling as a function of porosity. This means that under differential compressions a coating structure can create strongly varying absorption characteristics likely to affect print gloss and density without there being any changes in coating composition. This we suggest may be one of the dominant causes for print mottle in modern coated papers and supports the previous analysis of coating distribution and correlatable roughness given by Gane (2).
3. Associated with this transitional spread phenomenon is a further second potential discontinuity in coating layer absorption which may be related to the various stages of liquid content of pores. With increasing pore diameter a transition involving a mechanism of pore structure differentiation either between large and fine pores on a short timescale and/or pore draining after longer times may occur. This condition is further dependent on the pore-to-throat diameter ratio and the available volume of the smaller voids. Conversely, strongly divergent pores associated with highly porous structures may lead to a potential imbibition termination and leave some pores competitively unfilled. In the offset process where different volumes of contrasting fluids are used the discrepancy between the droplet volume exclusion case (limited volume) and the super source saturation effect (abundant volume) may account for differential absorption of fountain solution compared with ink in that, depending on the volume balance of the fluids and their properties, they may strongly compete for and access different pore volume.

Controlling the amount of potentially limited or competitive access of oil-based ink vehicles to the coating void structure due to the limited volume of fluid compared to the volume of coating pores together with the time retarding influence of viscosity may be a highly relevant factor in guaranteeing the correct balance between good ink acceptance (adhesion (20, 41)) and the need for long term stability of the ink layer against print rub and post-tack adhesion failure by extended ink tack cycle times (20).

It will be interesting to see, therefore, if the properties of different liquids can account for the discrepancy between equilibrium saturation of the pore structure and the exclusion of pore volume associated with limited fluid uptake. For example, is the polarity or higher viscosity of linseed oil likely to lead to an important difference compared with non-polar mineral oil of similar or lower viscosity in determining the printability of vegetable versus mineral oil-based inks in the case of non-equilibrium saturation? Dempewolf states that mineral oils (and *not* vegetable oils) are an indispensable component for slow setting sheet offset inks (42). Our finding that limited volumes of fluids may access a smaller pore volume at critical

porosity levels could be an explanation for differing imbibition rates or possible extended chromatography/setting of mineral oil compared with vegetable oil inks.

References

1 Engström G., Morin V. and Bin S. L., *"Analysis of porosity distribution in coating layers"*, Proceedings of the 1997 Tappi Advanced Coating Fundamentals Symposium, Tappi Press, Atlanta, p189-198

2 Gane P., *"Mottle and the influence of coating and binder migration"*, Paper Technology, PITA April 1989, p34-41

3 Zang Y. H. and Aspler J. S., *"Effect of binder content on print density and ink receptivity of coated paper"*, Journal of Pulp and Paper Science, 24(5), 1998, p141-145

4 Sangl R. and Weigl J., *"Forschungsbericht Inkjet"*, Papiertechnische Stiftung, München

5 Chapman D. M., *"Coating structure effects on ink-jet print quality"*, Proceedings of the 1997 Tappi Coating Conference, Tappi Press, Atlanta, p73-93

6 Arnold H., Eisenschmid K. and Kleemann S. G, *"Inkjet-Eignung von holzhaltigen Papieren"*, Wochenblatt für Papierfabrikation 123(21), 1995

7 Desjumaux D., Bousfield D. W., Glatter T. P., Donigian D. W., Ishley J. N. and Wise K. J., *"Influence of pigment size on wet ink gloss development"*, Journal of pulp and paper science, 24(5), 1998, p150-155

8 Donigian D. W., Ishley J. N. and Wise K. J., *"Coating structure and offset printed gloss"*, Tappi Journal, 80(5), 1997, p163-172

9 Plowman N., *"Ink tack - part 3: surface measurement"*, Gr. Arts. Mon. 61(6), 1989, p114
Plowman N., *"Ink tack - part 4: blanket release forces"*, Gr. Arts. Mon. 61(8), 1989, p133

10 Concannon P. W. and Wilson L. A., *"A method for measuring tack build of offset printing inks on caoted paper"*, TAGA Proc. 44, Vancouver, 1992

11 Piccolet M., Piette P., Morin V. and Le Nest J. F., *"Competition between gravure ink penetration and spreading on LWC coated papers"*, Proceedings of the 1998 Tappi Coating/Papermakers Conference New Orleans, Tappi Press Atlanta, p185-192

12 Abrams L., Favorite W., Capano J. and Johnson R. W., *"Using mercury porosimetry to characterize coating pore structure and its relevance to optical performance"* , Proceedings of the 1996 Tappi Coating Conference, Tappi Press Atlanta, p185-192

13 Larrondo L. E., St-Amour S. and Monasterios C., *"The porous structure of paper coatings - a comparison of mercury porosimetry and stain imbibition methods of measurement"*, Proceedings of the 1995 Tappi Coating Conference, Tappi Press, Atlanta, p79-93

14 Gane P., Kettle J., Matthews P. and Ridgway C., *"Void space of compressible polymer spheres and consolidated calcium carbonate paper coating formulations"*, Ind. Eng. Chem. Res. 1996, 35, p1753-1764

15 Bester P., Gerischer G., and Reinhardt B., *"Studium der Oberflächenveredlung von Spezialpapier mittels filmbildender Substanzen"*, Wochenblatt für Papierfabrikation, 11, 1994, p468-472

16 Lundqvist A., "*Surface energy characterisation of cellulosic fibres and pigment coatings by inverse gas chromatography (IGC)"*, Licentiate Thesis, STFI, Stockholm, 1996

17 Adamson A. W., "*Physical Chemistry of Surfaces"*, 5th Edition, A. Wyley Interscience Publication, New York (1990)

18 Holysz L. and Chibowski E, *"Surface free energy components of calcium carbonate and their changes due to radio frequency electric field treatment*", Journal of Colloid and Interface Science 164, p245-251 (1994)

19 Triantafillopoulos N., Lee D. and Philp D., *"Einfluss des Strichs auf das Wegschlagen beim Offsetdruck"*, Wochenblatt für Papierfabrikation, 4, 1997, p138-147

20 Gane P. A. C. and Seyler E. N., *"Some novel aspects of ink/paper interactions in offset printing"*, Proceedings of the 1994 International Printing and Graphic Arts Conference, Halifax, Nova Scotia, October 1994, CPPA/TAPPI, Tappi Press, Atlanta, p209-228

21 Järnström L., Lason L. and Rigdahl M., "*Strichstruktur und optische Eigenschaften gestrichener Papiere"*, Wochenblatt für Papierfabrikation, 17, 1996, p736-741

22 Larrondo L. E. and St-Amour S., "*A method for measuring the void fraction of coatings on porous substrates"*, J. Pulp and Paper Sci., Aug. 1994

23 Lepoutre P., Rezanovich A., "*Optical properties and structure of clay-latex coatings"*, Tappi 60(11), 86 (1977).

24 Leskinen A. M., "*Layer structure in model coatings"*, Tappi 70(12), p101-106 (1987)

25 Ranger A. E., "*Coating pore structure analysis by fluid penetration and permeation"*, BPBIF, Cambridge Symp., *„The role of fundamental research in papermaking*", 685, Sept. 1981.

26 Kettle J. P. and Matthews G. P., "*Computer modelling of the pore structure and permeability of pigmented coatings"*, Advanced Coating Fundamentals TAPPI Notes, 1993, p121-126

27 Unertl W. N., "*Wetting and spreading of styrene-butadiene latexes on calcite"*, Langmuir 1998, 14, p2201-2207

28 Sigg L., Goss K-U., Haderlein S., Harms H., Hug S. J., Ludwig C., "*Sorption phenomena at environmental solid surfaces"*, Chimia 51 (1997), p893-899

29 Stipp S. L. S, Gutmannsbauer W. and Lehmann T., *"The dynamic nature of calcite surfaces in air"*, American Mineralogist, Volume 81, p1-8, 1996

30 Kent H. J. and Lyne M. B., "*Influence of paper morphology on short term wetting and sorption phenomena"*, BPBIF Fundamental Research Symposium Cambridge, 895, Sept. 1989

31 Klemm K. W., "*Nachwachsende Rohstoffe in Offsetfarben"*, K+E Druckfarben PRINT, 14/15 (1994)

32 Hanke K., "*Oekologische Farbsysteme für den Bogenoffsetdruck"*, Deutscher Drucker 12/28(3), w30, 1996

33 Siegrist J., *"Sojaöl, Wunderwaffe für die europäischen Offsetdruckfarben"*, K+E Druckfarben PRINT 11 (1994)

34 Kittel H., *"Lehrbuch der Lacke und Beschichtungen"*, Band I, Teil3, Verlag W. A. Colomb, Berlin (1974)

35 Goldschmidt A., Hantschke B., Knappe E., and Vock G-F., *"Glasurit-Handbuch, Lacke und Farben"*, 11. Auflage, Curt R. Vincentz Verlag, Hannover (1984)

36 Pennanen M., "*Methods for producing and testing tablets of dry pigments and coating colours",* Research report, Åbo Akademi, Turku, OMYA, Oftringen, 1996

37 Ridgway C. J., Ridgway K. and Matthews G. P., "*Modelling of the void space of tablets compacted over a range of pressures"*, J. Pharm. Pharmacol. 49, (1997), p377

38 Briscoe B. J. and Rough S. L., "*Effects of wall friction in powder compaction"*, Colloids and Surfaces A., 137, p103-116, (1998)

39 Cook R. A. and Hover K. C., "*Mercury porosimetry of cement-based materials and associated correction factors"*, ACI Meter. J. March/April, p152-161 1993

40 Sangl R. and Weigl J., "*Cost-effective production of paper suitable for ink-jet printing at high production speeds"*, Research Report, Papiertechnische Stiftung, München

41 Haenen J. P., *"Ink-paper interaction, a new analysis for the control of back trap mottling"*, Proceedings of the PTS Coating Symposium 1999, Munich, 38-1, 14

42 Dempewolf E., *"Für Oekowerbung zu schade: Druckfarben mit nachwachsenden Rohstoffen"*, Polygraph, Treffpunkt Druckindustrie, 15/16 (1994)

43 Gane P.A.C., Schoelkopf J., Spielmann D.C., Matthews G.P. and Ridgway C.J., *"Observing fluid transport into porous coating structures: some novel findings"*, Proceedings of the Tappi Advanced Coating Fundamentals Symposium, Toronto, 1999, Tappi Press, Atlanta, 213-236.